# Magnetospheric electrodynamics

## Studying the Blandford/Znajek process in GR time evolution simulations of force-free electrodynamics around Kerr black holes

Jens F. Mahlmann, Pablo Cerdá-Durán, Miguel A. Aloy

Universitat de València
Departament d'Astronomia i Astrofísica (CAMAP)

CoCoNuT Meeting / Garching (Munich) / October 26, 2017

GENERALITAT VALENCIANA

European Research Council
Established by the European Commission

Studienstiftung des deutschen Volkes

# No clear picture from merger simulations

## Failing of jet launching despite favorable conditions

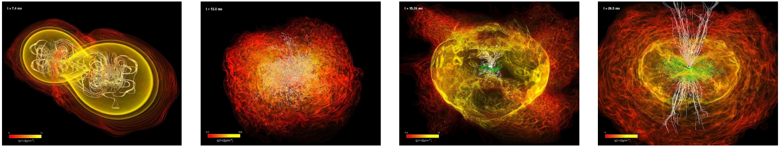

Figure: Simulation of the merger of two neutron stars (Rezzolla et al., 2011) with gravitational mass of 1.5 solar masses each during a time of 26.5 ms.

- Despite favorable conditions (e.g., magnetic fields) no jets clearly emerge after the BH formation (Rezzolla et al., 2011; Kiuchi et al., 2014). Simulations by Ruiz et al. (2016) did, however, discover jet launching.
- Possible explanations for missing jets: *Short simulation time* or *field reversals* observed over the low density funnel.

Current set of 'standard' magnetospheric field topologies (e.g., split-monopole, paraboloidal) may not be sufficient for time evolution simulations of the electromagnetic fields anymore.

# Blandford/Znajek explain jet powering I

## Creating a force-free black hole magnetosphere

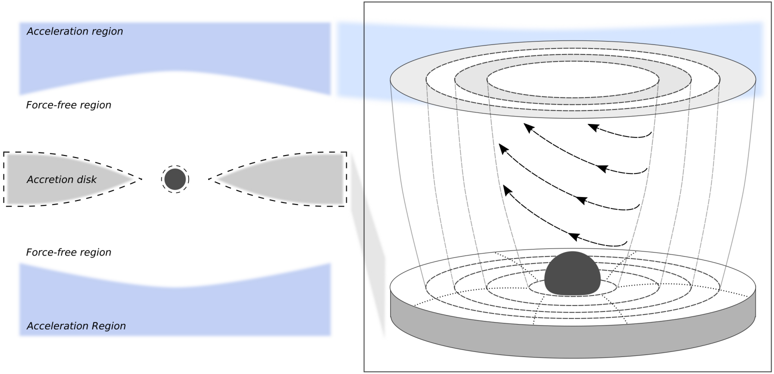


Figure: Schematic visualization of the Blandford/Znajek model (cf. MacDonald and Thorne, 1982). The black hole is embedded in a *force-free magnetosphere*. Magnetic fields are supported by a thin disc in the $\theta = \pi/2$ equatorial plane. The acceleration region which involves a break-down of the idealized conditions is set up at infinity and not considered for the derivations. A non-degenerate plasma generation region is schematically represented by the dashed lines.

# Blandford/Znajek explain jet powering II

## Spacetime magnetospheric electrodynamics

Blandford and Znajek (1977) intensively exploit the *covariant* form of the Maxwell equations in Kerr spacetime.

$$(*F^{\mu\nu})_{;\nu} = 0$$

$$\varepsilon_0^{-1} J^\mu = F^{\mu\nu}_{;\nu} = g^{-1/2}\left(g^{1/2} F^{\mu\nu}\right)_{,\nu}$$

$$F_{\mu\nu} = \mathcal{A}_{\nu,\mu} - \mathcal{A}_{\mu,\nu}$$

The existence of time-like and axial-like *symmetries* help to reduce the complexity of the resulting equations.

$$\mathcal{A}_{\mu,t} = \mathcal{A}_{\mu,\phi} = 0$$

$$\Longrightarrow F_{t\phi} = F_{\phi t} = 0$$

The *force-free condition* ultimately reduces to a differential equation governing the magnetosphere.

$$F_{\mu\nu} J^\nu = 0$$

$$\begin{aligned} 4\frac{\Sigma}{\Delta} I I' = &- \left(\frac{\Sigma - 2Mr}{\Sigma \sin\theta}\Psi_{,r}\right)_{,r} - \left(\frac{\Sigma - 2Mr}{\Delta\Sigma\sin\theta}\Psi_{,\theta}\right)_{,\theta} \\ &+ \omega^2\left\{\sin\theta\left(\frac{A}{\Sigma}\Psi_{,r}\right)_{,r} + \frac{1}{\Delta}\left(\frac{A\sin\theta}{\Sigma}\Psi_{,\theta}\right)_{,\theta}\right\} \\ &- 4Ma\omega\left\{\sin\theta\left(\frac{r\Psi_{,r}}{\Sigma}\right)_{,r} + \frac{r}{\Delta}\left(\frac{\sin\theta}{\Sigma}\Psi_{,\theta}\right)_{,\theta}\right\} \\ &+ \frac{\sin\theta}{\Sigma\Delta}\left(A\omega - 2Mar\right)\left(\Delta\left(\Psi_{,r}\right)^2 + \left(\Psi_{,\theta}\right)^2\right)\omega' \end{aligned}$$

- Second order non-linear elliptic PDE
- Singular surfaces (so called *light surfaces*)
- Mathematical treatment differs from the (analytical) approach in the neutron star case

# Numerics at the light surfaces I

## Close-up: Understanding the singular surfaces

Field quantities of the *3+1* decomposition (as measured by the *ZAMOs*) are required to stay finite. Lee et al. (2000) derive the following:

$$\rho = \left(\frac{\Omega - \omega}{4\pi^2 \alpha}\right) \frac{\frac{8\pi^2 I}{\alpha^2} \frac{\mathrm{d}I}{\mathrm{d}\Psi} - \boldsymbol{G} \cdot \nabla\Psi}{D}$$

$$\boldsymbol{j}_T = \left(\frac{1}{4\pi^2 \varpi}\right) \frac{\frac{8\pi^2 I}{\alpha^2} \frac{\mathrm{d}I}{\mathrm{d}\Psi} - \left(\frac{(\Omega-\omega)\varpi}{\alpha}\right)^2 \boldsymbol{G} \cdot \nabla\Psi}{D}$$

where $D$ denotes the light surface condition

$$D = 1 - \frac{(\omega - \Omega)^2\, \varpi^2}{\alpha^2}.$$

Smoothness of $\Psi$ throughout the magnetosphere is imposed as a regularity condition (as also used in, e.g., Contopoulos et al., 2013).

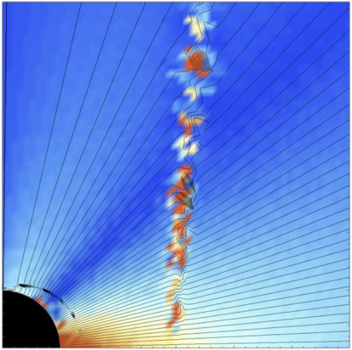

Figure: Numerical artifacts develop at the singular surfaces of the Grad-Shafranov equation. These breakings of field lines may cause the numerical solution to blow up.

**Strategy outline:** Ensure *smooth* passing through the light surfaces and reconstruct potential functions consistently.

# Numerics at the light surfaces II

## Close-up: Relaxation and smoothing procedures

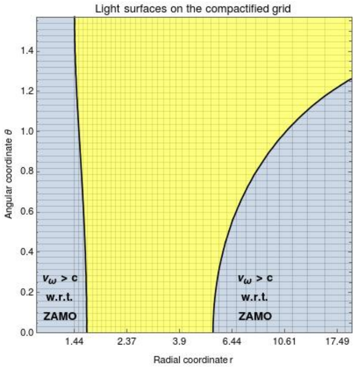


Figure: The light surfaces partition the domain into *three disconnected regions*. Their numerical interplay strongly affects the relaxation. At the location of the light surfaces (black lines), a *simplified Grad-Shafranov equation* can be solved (cf. Uzdensky, 2004) in order to relate the defining functions $\mathcal{A}_\phi$, $\omega$ and $I$.

### [1] Smoothing routines

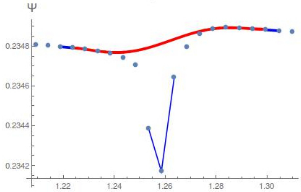


Figure: Visualization of the *smoothing* scheme applied at the light surfaces.

### [2] Adapted discretization

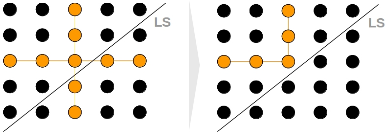


Figure: Visualization of the *biased stencil* introduced at the locations of the light surfaces (LS) in order to disconnect the domains in the discretization of first derivatives.

# Initial data for 3D FF simulations

## Obtaining mgnetospheric initial data from the GSE

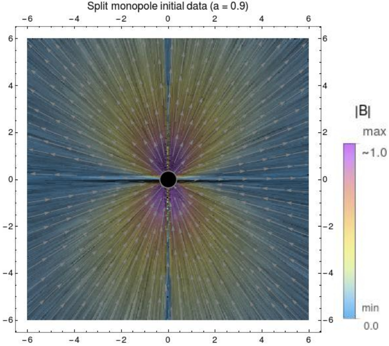


Figure: Visualization of the mag. field (**B**) initial data around the BH (mass $m = 1$, spin $a = 0.9$). A numerical solution to the Grad-Shafranov equation is obtained via the solver architecture in the *CoCoNut* code (cf. Adsuara et al., 2016) and as initial data for simulations employing the *Einstein Toolkit*.

- The numerical techniques solving the Grad-Shafranov equation around spinning Kerr BHs may be used with existing infrastructure of numerical PDE solvers, e.g., the *CoCoNut* code. (Cerdá-Durán et al., 2009; Adsuara et al., 2016)
- Spacetime initial data for rapidly spinning BHs (high Blandford/Znajek luminosities expected) is tested on the *Carpet* grid of the *Einstein Toolkit*. (Liu et al., 2009)
- We have adapted the evolution routines available for the ET to account for a FF magnetized plasma around spinning BHs implemented as *punctures*. Our implementation is inspired by previous work on GRMHD using the ET and GRFFE. (Faber et al., 2007; Mösta et al., 2014; Etienne et al., 2017)

# Time evolution of FF electrodynamics I

## Comparison of evolution schemes

### [1] Full Maxwell's equations evolution

(Komissarov, 2002, 2004, 2007; Paschalidis and Shapiro, 2013)

$$\nabla_\nu F^{\mu\nu} = J^\mu \qquad \nabla_\nu {}^*F^{\mu\nu} = 0$$

*Augmented system*

(Dedner et al., 2002; Palenzuela et al., 2009; Mignone and Tzeferacos, 2010)

$$\nabla_\nu\left({}^*F^{\mu\nu} + \left({c_h}^2\gamma^{\mu\nu} - n^\mu n^\nu\right)\psi\right) = -\kappa_\psi k^\mu \psi$$
$$\nabla_\nu\left(F^{\mu\nu} + g^{\mu\nu}\phi\right) = J^\mu - \kappa_\phi k^\mu \phi$$

### [2] Energy flow evolution

(McKinney, 2006; Paschalidis and Shapiro, 2013; Etienne et al., 2017)

$$\nabla_\mu T^\mu{}_\nu = 0 \qquad \nabla_\nu {}^*F^{\mu\nu} = 0$$

*Augmented system*

(Dedner et al., 2002; Palenzuela et al., 2009; Mignone and Tzeferacos, 2010)

$$\nabla_\nu\left({}^*F^{\mu\nu} + \left({c_h}^2\gamma^{\mu\nu} - n^\mu n^\nu\right)\psi\right) = -\kappa_\psi k^\mu \psi$$

The div$\mathbf{B} = 0$ and div$\mathbf{D} = \rho$ constraints are ensured by a mixed *hyperbolic/parabolic* correction with the additional scalar potentials $\psi$ and $\phi$. In its analogy to the *telegraph equation*, the factor $c_h$ is the finite propagation speed of divergence errors, the constants $\kappa_\psi$ and $\kappa_\phi$ are their damping rate. The above equations are formulated in a *conserved flux formulation*:

$$\partial_t \mathcal{C} + \partial_j \mathcal{F}^j = \mathcal{S}_n + \mathcal{S}_s$$

# Time evolution of FF electrodynamics II

## Conserved flux formulation (dynamic spacetimes)

**[1] Full Maxwell's equations evolution**

- Requires *(force-free) currents* (cf. Komissarov, 2011)
- Fluxes derived from *conserved* quantities

$$\mathcal{C} \equiv \gamma \begin{pmatrix} \frac{\psi}{\alpha} \\ \frac{\phi}{\alpha} \\ B^i + \frac{\psi}{\alpha}\beta^i \\ D^i - \frac{\phi}{\alpha}\beta^i \end{pmatrix} \qquad \mathcal{F}^j \equiv \gamma \begin{pmatrix} B^j - \frac{\psi}{\alpha}\beta^i \\ -\left(D^j + \frac{\phi}{\alpha}\beta^i\right) \\ e^{ijk}E_k + \alpha\left({c_h}^2\gamma^{ij} - n^i n^j\right)\psi \\ -\left(e^{ijk}H_k + \alpha g^{ij}\phi\right) \end{pmatrix}$$

$$\mathcal{S}_n \equiv \begin{pmatrix} -\gamma\alpha\psi\,\Gamma^t_{\alpha\beta}\left({c_h}^2\gamma^{\alpha\beta} - n^\alpha n^\beta\right) \\ -\gamma\alpha\phi\Gamma^t_{\alpha\beta}g^{\alpha\beta} - \gamma\rho \\ -\psi\left[\alpha\gamma\Gamma^i_{\alpha\beta}\left({c_h}^2\gamma^{\alpha\beta} - n^\alpha n^\beta\right)\right] \\ -\gamma\alpha\phi\Gamma^i_{\alpha\beta}g^{\alpha\beta} - \gamma J^i \end{pmatrix} \qquad \mathcal{S}_s \equiv \begin{pmatrix} -\alpha\gamma\kappa_\psi\psi \\ -\alpha\gamma\kappa_\phi\phi \\ 0 \\ 0 \end{pmatrix}$$

**[2] Energy flow evolution**

- $\mathbf{D}$ is reconstructed ($\mathbf{D}\cdot\mathbf{B} = 0$)
- Fluxes derived from *primitive* quantities

$$\mathcal{C} \equiv= \gamma \begin{pmatrix} \frac{\psi}{\alpha} \\ B^i + \frac{\psi}{\alpha}\beta^i \\ \alpha {T^t}_i \end{pmatrix} \qquad \mathcal{F}^j \equiv \gamma \begin{pmatrix} B^j - \frac{\psi}{\alpha}\beta^i \\ e^{ijk}E_k + \alpha\left({c_h}^2\gamma^{ij} - n^i n^j\right)\psi \\ \alpha {T^i}_j \end{pmatrix}$$

$$\mathcal{S}_n \equiv \begin{pmatrix} --\gamma\alpha\psi\,\Gamma^t_{\alpha\beta}\left({c_h}^2\gamma^{\alpha\beta} - n^\alpha n^\beta\right) \\ -\psi\left[\alpha\gamma\Gamma^i_{\alpha\beta}\left({c_h}^2\gamma^{\alpha\beta} - n^\alpha n^\beta\right)\right] \\ \frac{1}{2}\alpha g_{\mu\nu,i}\,T^{\mu\nu} \end{pmatrix} \qquad \mathcal{S}_s \equiv \begin{pmatrix} -\alpha\gamma\kappa_\psi\psi \\ 0 \\ 0 \end{pmatrix}$$

# Maintaining a force-free magnetosphere

## Preservation of force-free constraints

GRFFE can be considered as the limit of *vanishing particle inertia* of GRMHD (cf. Komissarov, 2011). In GRFFE the following independent constraints hold:

$$^{*}F_{\mu\nu}F^{\mu\nu} = 0 \qquad \mathbf{D} \perp \mathbf{B}$$

$$F_{\mu\nu}F^{\mu\nu} > 0 \qquad \mathbf{B}^2 - \mathbf{D}^2 > 0$$

These conditions are **not** automatically fulfilled (e.g., at the location of *current sheets*) but ensured, e.g., by:

- Numerical *cutback* of violations
  (Palenzuela et al., 2010; Alic et al., 2012)
- Addition of suitable dissipation by *driver terms*
  (Komissarov, 2004, 2011; Alic et al., 2012; Parfrey et al., 2017)
- Limitation of constraint violations to *narrow regions*
  (Parfrey et al., 2017)

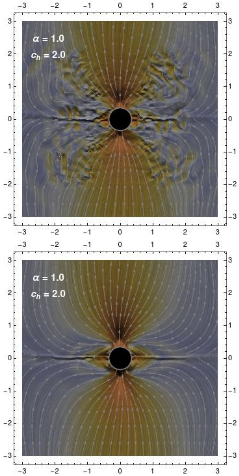


Figure: Test runs of the *energy flow evolution* without numerical cutback of **D** ⊥ **B** violations (*top*) and with the respective corrections employed in every *Con2Prim* step (*bottom*).

Publication in preparation (2018)

# Divergence cleaning optimization AI

## Parameter adjustment for $c_h$ and $\kappa_\psi$

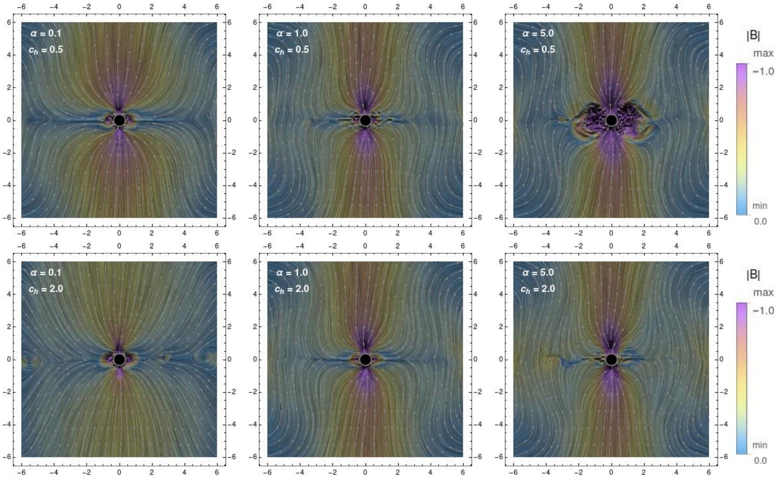


Figure: Visualization of the magnetic field (**B**) around a puncture BH (mass $m = 1$, spin $a = 0.9$) for selected test cases after an evolution of the *energy flow* scheme for $t = 15M$.

*Publication in preparation (2018)*

# Divergence cleaning optimization AII

## Parameter adjustment for $c_h$ and $\kappa_\psi$

Figure: Close-up on the magnetic field (**B**) configuration for $c_h = 2.0$, and $\alpha = 1.0$ close to the black hole (mass $m = 1$, spin $a = 0.9$) after the evolution with the *energy flow* scheme after $t = 15M$. This selected test case minimizes the divergence error throughout the evolution.

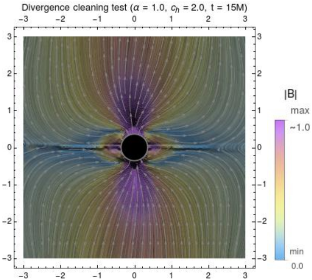


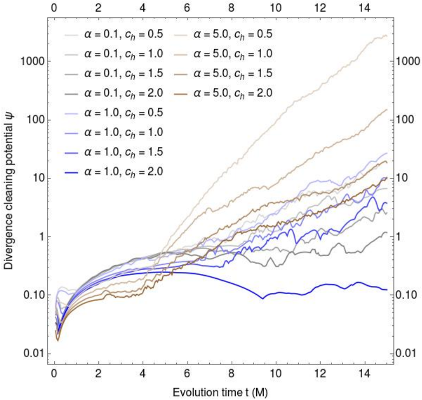


Figure: Evolution of the maximum of the divergence cleaning potential max $\psi$ outside of the outer event horizon for selected test cases ($t = 15M$) with different choices of the parameters $c_h$ (propagating speed of divergence errors) and $\kappa_\psi$ (damping rate of divergence errors).

*Publication in preparation (2018)*

# Divergence cleaning optimization BI

## Parameter adjustment for $c_h$ and $\kappa_\psi$

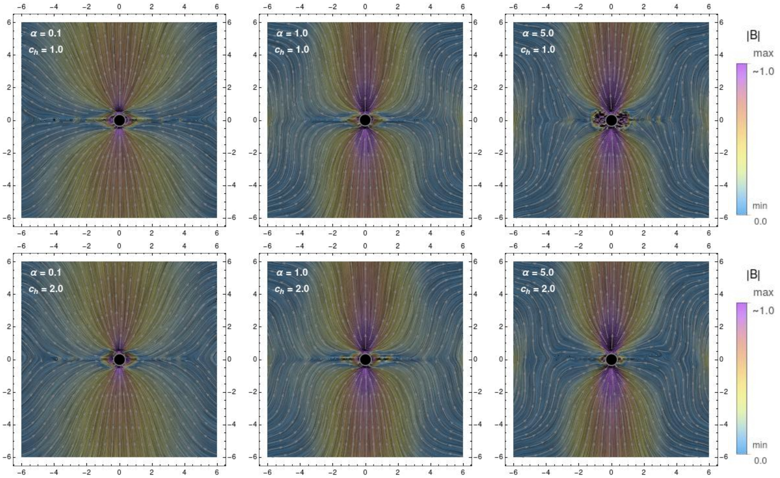


Figure: Visualization of the magnetic field (**B**) around a puncture BH (mass $m = 1$, spin $a = 0.9$) for selected test cases after an evolution of the *full Maxwell's equation* scheme for $t = 15M$.

# Divergence cleaning optimization BII

## Parameter adjustment for $c_h$ and $\kappa_\psi$

Figure: Close-up on the magnetic field ($\mathbf{B}$) configuration for $c_h = 2.0$, and $\alpha = 1.0$ close to the black hole (mass $m = 1$, spin $a = 0.9$) after the evolution with the *full Maxwell's equation* scheme after $t = 15M$. This selected test case minimizes the divergence error throughout the evolution.

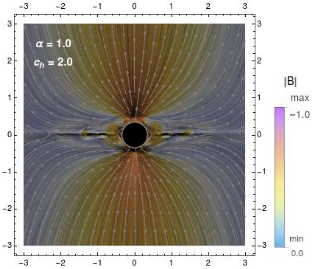


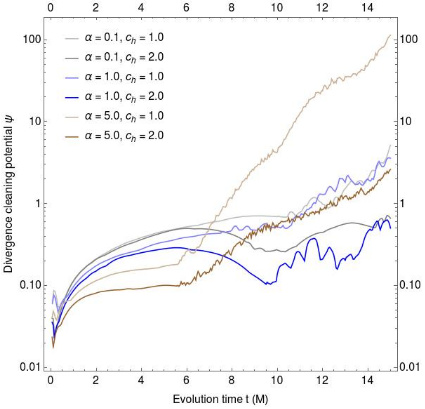


Figure: Evolution of the maximum of the divergence cleaning potential $\max \psi$ outside of the outer event horizon for selected test cases ($t = 15M$) with different choices of the parameters $c_h$ (propagation speed of divergence errors) and $\kappa_\psi$ (damping rate of divergence errors).

# Outlook: Research stages and methods

## Numerical simulations as astrophysical experiments

### Stage I: **Theory/Numerics**

Grad-Shafranov initial data

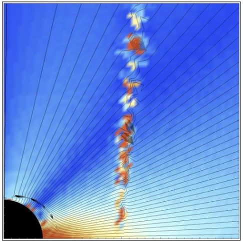

- Implementation and testing of a numerical solving procedure for the GS equation.
- *Expand solving scheme towards more complicated field topologies.*

### Stage II: **Simulations**

Einstein Toolkit setup

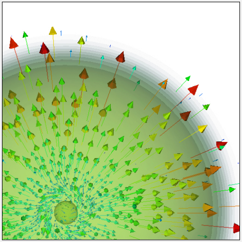

- Preparation of GS solutions as initial data for time evolution setups.
- *Adaptation of a suitable evolution scheme (employing the Einstein Toolkit).*

### Stage III: **Evaluation/Feedback**

Fortran code segment

```
call Compute_Function_Value(PsiGrid(i,j,k), ITmp
! Linear operator coefficients >>>>>>>>>>>>>>>>>
! Linear terms from BZ77 - Simplified in Mathemat
c1(1,1,i,j,k) = (1.0d0/SigmaBL**2.0d0)* &
     (2.0d0*bhspin_sq*cBL_sq*(bhmass+OmegaTmp*sBL
     bhspin_sq*(bhmass-rBL)*OmegaTmp*sBL_sq))+ &
     2.0d0*rBL*((-bhmass)*rBL+OmegaTmp*sBL_sq*(2
c11(1,1,i,j,k) = ((2.0d0*bhmass-rBL)*rBL-bhspin_
     bhspin_sq*(bhspin_sq-2.0d0*bhmass*rBL+rBL_s
c2(1,1,i,j,k) = (32.0d0*(bhspin_sq+rBL_sq)*Delta
     (-8.0d0*bhspin_sq*(3.0d0*bhspin_sq+4.0d0*rBL
     (5.0d0*bhspin**6.0d0+16.0d0*rBL**6.0d0+16.0
     4.0d0*bhspin_sq*(-bhspin_sq+4.0d0*bhspin*bh
     sin(4.0d0*theta(j))+bhspin**4.0d0*DeltaBL*O
     (32.0d0*DeltaBL*SigmaBL**2.0d0)
c22(1,1,i,j,k) = ((2.0d0*bhmass-rBL)*rBL-bhspin_
     bhspin_sq*(bhspin_sq-2.0d0*bhmass*rBL+rBL_s

! Non-linear operator coefficients >>>>>>>>>>>>>
! Non-linear terms from BZ77 - Simplified in Math
if ((i.lt.1).or.(i.gt.m).or.(j.lt.1).or.(j.gt.n)
   Source(i,j,k)=0.0d0
else
   Source(i,j,k)= (-((sBL_sq)*(-2.0d0*bhspin*bhma
```

- *Classify GS initial data in terms of stability and the observation of jet launching.*
- *Understand the role of force-free evolution vs. ideal MHD implementations.*

# Open forum: Let's discuss

Questions. Answers. Remarks. Discussion.

**Thank you.**

GENERALITAT VALENCIANA

erc
European Research Council
Established by the European Commission

Studienstiftung des deutschen Volkes

# References I

J. E. Adsuara, I. Cordero-Carrión, P. Cerdá-Durán, and M. A. Aloy. Scheduled Relaxation Jacobi method: Improvements and applications. *Journal of Computational Physics*, 321:369–413, Sept. 2016. doi:10.1016/j.jcp.2016.05.053.

D. Alic, P. Moesta, L. Rezzolla, O. Zanotti, and J. L. Jaramillo. Accurate Simulations of Binary Black Hole Mergers in Force-free Electrodynamics. *ApJ*, 754:36, July 2012. doi:10.1088/0004-637X/754/1/36.

R. D. Blandford and R. L. Znajek. Electromagnetic extraction of energy from Kerr black holes. *MNRAS*, 179 (3):433–456, 1977. doi:10.1093/mnras/179.3.433.

P. Cerdá-Durán, N. Stergioulas, and J. A. Font. Alfvén QPOs in magnetars in the anelastic approximation. *MNRAS*, 397(3):1607–1620, 2009. doi:10.1111/j.1365-2966.2009.15056.x.

I. Contopoulos, D. Kazanas, and D. B. Papadopoulos. The force-free magnetosphere of a rotating black hole. *ApJ*, 765(2):113, 2013. doi:10.1088/0004-637x/765/2/113.

A. Dedner, F. Kemm, D. Kröner, C.-D. Munz, T. Schnitzer, and M. Wesenberg. Hyperbolic Divergence Cleaning for the MHD Equations. *Journal of Computational Physics*, 175:645–673, Jan. 2002. doi:10.1006/jcph.2001.6961.

Z. B. Etienne, M.-B. Wan, M. C. Babiuc, S. T. McWilliams, and A. Choudhary. Giraffe: An open-source general relativistic force-free electrodynamics code. 2017.

J. A. Faber, T. W. Baumgarte, Z. B. Etienne, S. L. Shapiro, and K. Taniguchi. Relativistic hydrodynamics in the presence of puncture black holes. *Phys. Rev. D*, 76(10), 2007. doi:10.1103/physrevd.76.104021.

K. Kiuchi, K. Kyutoku, Y. Sekiguchi, M. Shibata, and T. Wada. High resolution numerical relativity simulations for the merger of binary magnetized neutron stars. *Phys. Rev. D*, 90(4), 2014. doi:10.1103/physrevd.90.041502.

S. S. Komissarov. Time-dependent, force-free, degenerate electrodynamics. *MNRAS*, 336(3):759–766, 2002. doi:10.1046/j.1365-8711.2002.05313.x.

S. S. Komissarov. Electrodynamics of black hole magnetospheres. *MNRAS*, 350(2):427–448, 2004. doi:10.1111/j.1365-2966.2004.07598.x.

S. S. Komissarov. Multidimensional numerical scheme for resistive relativistic magnetohydrodynamics. *MNRAS*, 382:995–1004, Dec. 2007. doi:10.1111/j.1365-2966.2007.12448.x.

# References II

S. S. Komissarov. 3+1 magnetodynamics. *MNRAS*, 418:L94–L98, Nov. 2011. doi:10.1111/j.1745-3933.2011.01150.x.

H. K. Lee, R. Wijers, and G. Brown. The Blandford-Znajek process as a central engine for a gamma-ray burst. *Physics Reports*, 325(3):83–114, 2000. doi:10.1016/s0370-1573(99)00084-8.

Y. T. Liu, Z. B. Etienne, and S. L. Shapiro. Evolution of near-extremal-spin black holes using the moving puncture technique. *Phys. Rev. D*, 80(12), 2009. doi:10.1103/physrevd.80.121503.

D. MacDonald and K. S. Thorne. Black-hole electrodynamics: an absolute-space/universal-time formulation. *MNRAS*, 198(2):345–382, 1982. doi:10.1093/mnras/198.2.345.

J. C. McKinney. General relativistic force-free electrodynamics: a new code and applications to black hole magnetospheres. *MNRAS*, 367:1797–1807, Apr. 2006. doi:10.1111/j.1365-2966.2006.10087.x.

A. Mignone and P. Tzeferacos. A second-order unsplit Godunov scheme for cell-centered MHD: The CTU-GLM scheme. *J. Comput. Phys.*, 229:2117–2138, 2010. doi:10.1016/j.jcp.2009.11.026.

P. Mösta, B. C. Mundim, J. A. Faber, R. Haas, S. C. Noble, T. Bode, F. Löffler, C. D. Ott, C. Reisswig, and E. Schnetter. GRHydro: a new open-source general-relativistic magnetohydrodynamics code for the Einstein toolkit. *Classical and Quantum Gravity*, 31(1):015005, Jan. 2014. doi:10.1088/0264-9381/31/1/015005.

C. Palenzuela, L. Lehner, O. Reula, and L. Rezzolla. Beyond ideal MHD: towards a more realistic modelling of relativistic astrophysical plasmas. *MNRAS*, 394:1727–1740, 2009. doi:10.1111/j.1365-2966.2009.14454.x.

C. Palenzuela, T. Garrett, L. Lehner, and S. L. Liebling. Magnetospheres of black hole systems in force-free plasma. *Phys. Rev. D*, 82(4):044045, Aug. 2010. doi:10.1103/PhysRevD.82.044045.

K. Parfrey, A. Spitkovsky, and A. M. Beloborodov. Simulations of the magnetospheres of accreting millisecond pulsars. *MNRAS*, 469:3656–3669, 2017. doi:10.1093/mnras/stx950.

V. Paschalidis and S. L. Shapiro. A new scheme for matching general relativistic ideal magnetohydrodynamics to its force-free limit. *Phys. Rev. D*, 88(10):104031, Nov. 2013. doi:10.1103/PhysRevD.88.104031.

L. Rezzolla, B. Giacomazzo, L. Baiotti, J. Granot, C. Kouveliotou, and M. A. Aloy. The missing link: Merging neutron stars naturally produce jet-like structures and can power short gamma-ray bursts. *ApJ*, 732(1): L6, 2011. doi:10.1088/2041-8205/732/1/l6.

M. Ruiz, R. N. Lang, V. Paschalidis, and S. L. Shapiro. Binary Neutron Star Mergers: A Jet Engine for Short Gamma-Ray Bursts. *ApJL*, 824:L6, June 2016. doi:10.3847/2041-8205/824/1/L6.

D. A. Uzdensky. Force-free magnetosphere of an accretion disk - black hole system. I. schwarzschild geometry. *ApJ*, 603(2):652–662, 2004. doi:10.1086/381543.